

No-flux boundaries stabilize scroll rings in excitable media with negative filament tension

Arash Azhand¹, Rico Buchholz², Florian Buchholz¹, Jan F. Totz¹, Harald Engel^{1*}

¹*Institut für Theoretische Physik, Technische Universität Berlin, Hardenbergstrasse 36, D-10623 Berlin, Germany*

²*Theoretische Physik V, Universität Bayreuth, Universitätsstrasse 30, D-95440 Bayreuth, Germany*

Scroll rings in an unbounded excitable medium with negative line tension undergo an instability ending eventually in a “turbulent” state, known as scroll wave (Winfree) turbulence. In this paper we demonstrate by numerical simulations based upon the Oregonator model for the photosensitive Belousov-Zhabotinskii reaction (PBZR) that the Winfree turbulence is suppressed by the interaction of the scroll ring with a confining Neumann boundary. Instead of the Winfree turbulence a stable scroll ring forms due to the boundary interaction. Furthermore, we will discuss the conditions under which boundary-stabilized scroll rings could be observed in the PBZR, taking into account a light-induced excitability gradient in parallel to the scroll ring’s symmetry axis.

I. INTRODUCTION

Excitable media can be found in many parts of biology and physics. Under non-equilibrium conditions pattern formation can appear in many of those systems. A common pattern that may develop is the spiral wave. It has been observed in slime molds [1], on platinum surfaces [2], chemical systems [3] and in the heart [4].

Some parts of the human heart tissue, especially at the ventricles, are thick enough to support not only spirals, but also three dimensional structures, for example scroll waves and scroll rings. This makes an investigation of these structures important, too.

The heart tissue can provide three dimensional structures, but the boundaries are never too far away. Because of this not only the evolution of spirals and scrolls in an unbounded domain need to be known but also the interaction with the boundary. For spirals the interaction with straight and circular boundaries is well studied [5–8]. The interaction of scroll waves and scroll rings with one or more no-flux boundaries is less discovered.

The first experimental observation of scroll rings was reported by Winfree [9] in the framework of the Belousov-Zhabotinskii reaction. Later scroll rings were also observed in fibrillating cardiac tissue [10].

One of the most important questions here is dealing with the time-evolution of scroll rings, that is whether the radius of the ring is shrinking (“positive filament tension”) or expanding (“negative filament tension”) in time. Several experimental [11–14] and theoretical [15–17] studies revealed the dynamics of contracting scroll rings.

The primary numerical prediction of scroll rings with negative filament tension was reported by Panfilov and Rudenko [18]. In experiments scroll rings with negative filament tension were found by Bánsági and Steinbock [19], who were also able to determine the tension of the filament. Later a connection to negative tension instability (Winfree turbulence) was drawn by Alonso et al. [20] and Zaritski and colleagues [21]. Alonso and col-

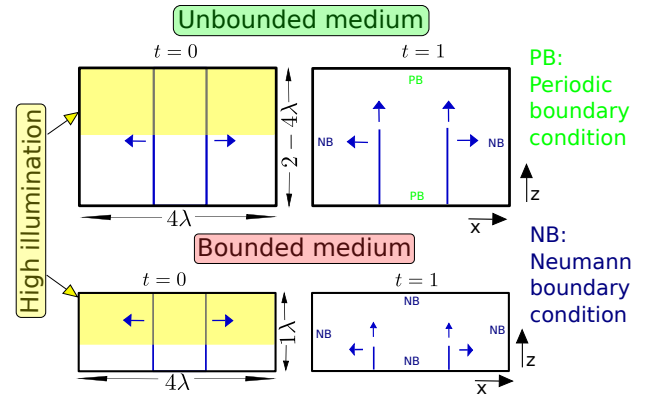


Figure 1. Schematic illustration for numerical initiation of scroll rings in unbounded and bounded media.

leagues were also able to suppress this turbulent state by applying periodic forcing [20, 22].

Investigation of scroll rings in excitable media with inhomogeneities were accomplished by application of parameter gradients, such as gradients of light in the photosensitive BZ reaction [23] or by applying gradients of temperature in the Ferroin catalyzed BZR [24, 25].

Nandapurkar and Winfree [26] for the first time found a stable scroll ring at a no-flux boundary through numerical investigations of the FitzHugh-Nagumo (FHN) model in the negative filament tension parameter regime.

Bray and Wikswow [27] studied the interaction of two contracting scroll rings in a symmetric configuration, which is equivalent to the situation of one scroll ring that interacts with a Neumann boundary.

The present work is now devoted to a systematic numerical study of boundary-stabilized scroll rings with negative filament tension, both in homogeneous and non-homogeneous excitable media.

The structure of this paper is as follows. First we introduce in section II the model that we used for the numerical simulations. A brief summary of scroll ring filament dynamics in unbounded media is given in sec-

tion III. In the subsequent section (sec. IV) we show how these dynamics change due to the interaction with a Neumann boundary and then address the question if the scroll rings remain stable for reasonable timescales (more than 100 rotation periods of corresponding spiral waves). In Section V we will show that observation of boundary-stabilized expanding scroll rings in the framework of the photosensitive Belousov-Zhabotinskii reaction (PBZR) may be possible. This includes an investigation of scroll ring initiation under variation of media thickness versus intensity of photoinhibition (subsection VA), evolution of boundary-stabilized scroll rings in media with different degrees of inhomogeneity (subsection VB), and stability of the scroll ring when initiated with different degrees of inclination (subsection VC). Finally, section VI is devoted to a short conclusion.

II. MODEL

In order to simulate realistic behaviour of scroll rings in thin layers of photosensitive BZ media, we used the "modified complete Oregonator model" [28, 29],

$$\begin{aligned} \frac{\partial u}{\partial t} &= \frac{1}{\epsilon_u} (u - u^2 + w(q - u)) + D_u \Delta u \\ \frac{\partial v}{\partial t} &= u - v \\ \frac{\partial w}{\partial t} &= \frac{1}{\epsilon_w} (\phi + fv - w(q + u)) + D_w \Delta w, \end{aligned} \quad (1)$$

where u , v and w are proportional to concentrations of HBrO_2 (activator), $\text{Ru}(\text{bpy})_3^{3+}$ (oxidized form of the catalyst) and Br^- (inhibitor), respectively. Δ is the Laplacian operator, diffusion coefficients will be chosen as $D_u = 1.0$ for activator u , $D_w = 1.12$ for inhibitor w , while there will be no diffusion for the catalyst v since in experiments the catalyst $\text{Ru}(\text{bpy})_3^{3+}$ is immobilized in a gel layer.

Parameters of the model are given by the recipe-dependent time scales ϵ_u and ϵ_w with $\epsilon_u \gg \epsilon_w$, ratio of rate constants q , stoichiometric parameter f , and photochemically induced bromide flow ϕ that is assumed to be proportional to applied light intensity.

We have chosen parameter sets that are shown in table I.

A two dimensional spiral has a period of $T = 6.8$ t.u. and a wavelength of $\lambda = 22.6$ s.u. for the parameter set 1 while for set 2 spirals exhibit a period of $T = 6.9$ t.u. and a wavelength of $\lambda = 19.6$ s.u.

In both parameter sets spiral waves perform rigidly rotating spiral tip motion. While parameter set 1 shows a transition of spiral tip motion from outward meander via inward meander to rigid rotation as one varies ϕ from

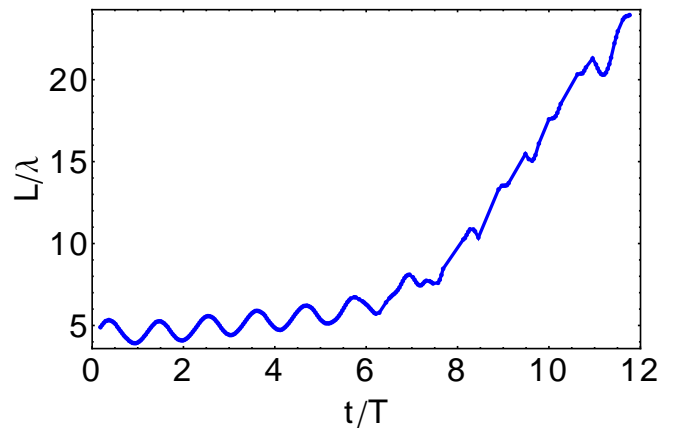


Figure 2. Evolution of filament length for a scroll ring propagating in an unbounded medium and parameter set 1. Parameter values are $\epsilon_u = 0.07$, $\epsilon_w = \epsilon_u/90$, $f = 1.4$, $q = 0.002$, and $\phi = 0.023$.

lower to higher values, in parameter set 2 one observes only rigid rotation, no matter which value of ϕ is chosen.

Simulations were conducted with an Euler scheme for time integration and a nineteen point star discretization of the laplacian. For space and time discretization we used $dx = dy = dz = 0.3$ and $dt = 0.0005$, respectively. Conditions for spatial geometry were always chosen such that unbounded scroll rings could evolve in 'boxes' of $4 \times 4 \times 2\lambda^3$ while confined scroll rings were placed into 'boxes' with $4 \times 4 \times 1\lambda^3$ (see Fig. 1). Neumann boundary conditions were chosen for all sides of the medium in case of bounded media while for the top and bottom boundaries periodic boundary conditions were used for unbounded media.

Initiation of scroll rings in unbounded and bounded media were accomplished in two steps. First we prepared outwardly propagating cylindric waves of different radii as initial conditions while the height of cylinders were reaching from bottom to top of corresponding media (from $z = z_{\text{bottom}} \equiv 0$ to $z = z_{\text{top}}$). Secondly, in a cuboidal part of corresponding media the photochemically induced bromide flow ϕ was set to a large value ($\phi = 0.2$), in order to inhibit wave propagation in these regions, starting at simulation time $t = 0$ and resetting ϕ homogeneously to standard values (sets 1 and 2) at time

Table I. Parameter sets one and two that were investigated numerically in this publication.

Parameter set	1	2
ϵ_u	0.07	0.07
ϵ_w	$\epsilon_u/90$	$\epsilon_u/90$
f	1.4	1.16
q	0.002	0.002
ϕ	0.023	0.014

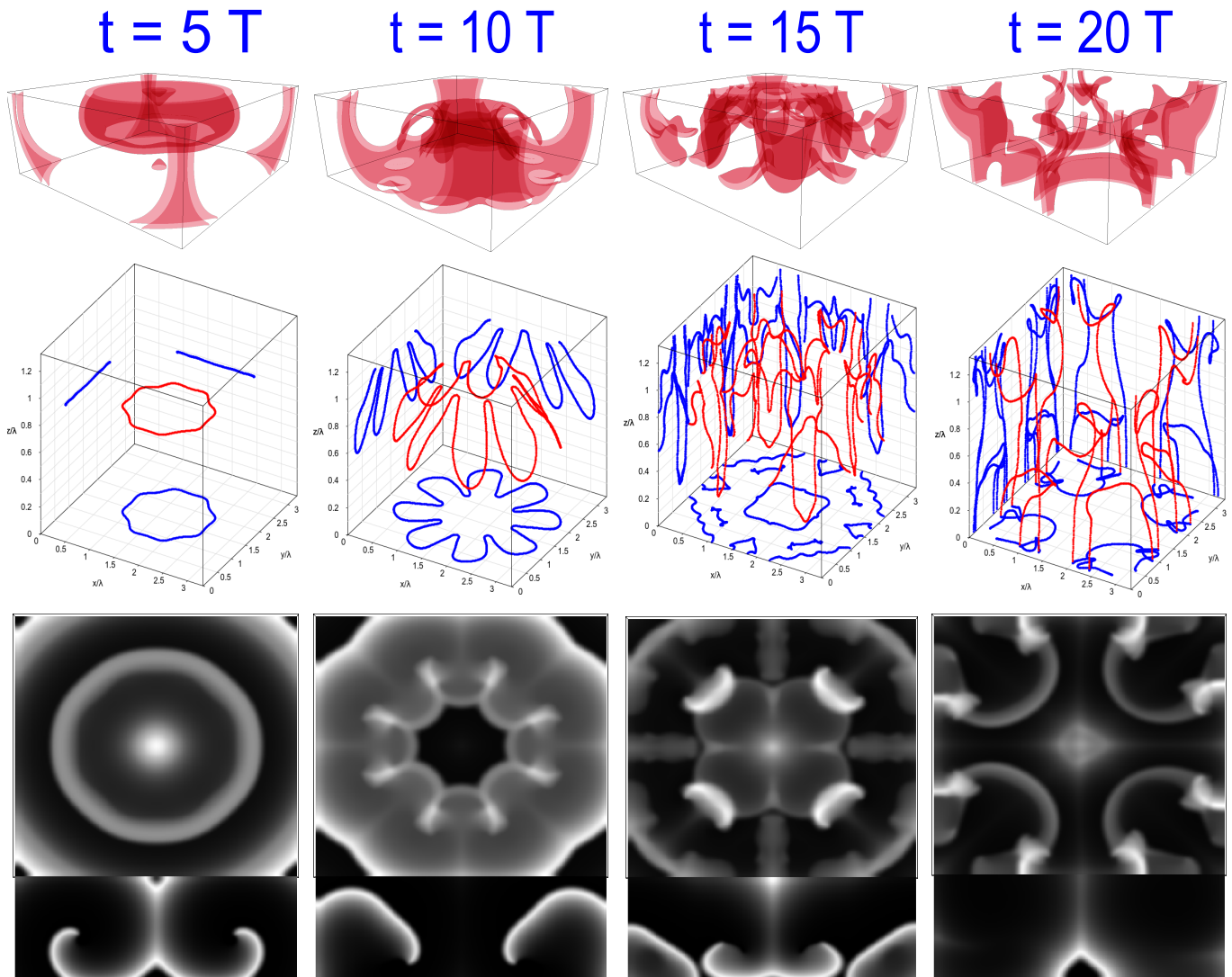


Figure 3. Multiple view panels for a scroll ring in an unbounded medium: perspective, filament, top, and side view (from top to bottom of figure). Perspective view displays the isosurfaces for Oregonator variable $u = 0.2$, filament view is showing the filament (red) and its projections into the different planes (blue), while the top view illustrates the overall concentration of Oregonator variable v as a sum over medium height (as may be seen by an observer of an experiment in the PBZR when looking from top). Figure displays destabilization of the filament due to negative filament tension instability. The initially planar circular filament is distorted ($t = 5T$), the modulations increase ($t = 10T$), and finally the filament fragments into pieces ($t = 15T$). The cascade results in a spatio-temporally irregular wave pattern known as Winfree-turbulence. Parameters as in Fig. 2.

$t = 1$. After resetting the medium the remained half cylindrical waves could evolve into perfectly planar scroll rings.

Both in unbounded and bounded media the cuboidal region in which the wave propagation was inhibited was chosen to be the upper part of the media (see Fig. 1). For unbounded media this region comprised half of the whole medium while for bounded media the cuboidal region was chosen such that the initial plane of corresponding scroll ring filaments were located approximately 0.2λ from the lower Neumann boundary.

The filament was defined via the crossing of two isosur-

faces, namely $u_f = 0.3$ and $v_f = 0.1$ that is the definition of the instantaneous filament. This definition leads to an oscillation of the filament position in time.

III. SCROLL RING DYNAMICS IN UNBOUNDED MEDIA

Far from any boundary the dynamics of a free scroll ring in homogeneous media is governed by the equations [16, 17]

$$\frac{dR}{dt} = -\frac{\alpha}{R}, \quad (2)$$

$$\frac{dz}{dt} = \frac{\beta}{R}, \quad (3)$$

where α and β are constants. Solutions to equations (2) and (3) are given by

$$R(t) = \sqrt{R_0^2 - 2\alpha t}, \quad (4)$$

$$z(t) = z_0 - \frac{\beta}{\alpha} R(t). \quad (5)$$

The filament tension α determines whether the scroll ring shrinks ($\alpha > 0$) or expands ($\alpha < 0$). A wave with closed filament and positive line tension would finally collapse while an open filament would straighten. In both cases small distortions decay. If the filament tension is negative, a scroll ring will grow. A straight/circular filament would not remain straight/circular, but small distortions will grow comparably faster, because of the radius dependence. This is the negative line tension instability that leads to Winfree turbulence [20–22]. The second parameter, β , leads to a constant drift parallel to the symmetry axis of the ring.

We calculated filament tension α and drift coefficient β for the chosen parameter sets by fitting equations 4 and 5 to the corresponding filament data from the numerical simulations. Results are shown in table II.

Evolution of the scroll ring is shown in figure 3. The initially circular filament starts to evolve small deviations that grow due to the negative filament tension instability ($t = 5T$ to $t = 10T$). Finally the filament fragments into pieces ($t = 15T$). Each single fragment grows further due to the instability ($t = 20T$). When each of these single filaments touch one of the boundaries, they start to fragment further until the whole medium is loaded with filament fragments. This is known as scroll wave (or Winfree) turbulence [20–22].

Table II. Calculated values with asymptotic standard errors for filament tension α and vertical drift coefficient β by fitting equations (4) and (5) to the corresponding filament data from the numerical simulations of scroll rings in unbounded media.

Parameter set	1	2
$R_0 [\lambda]$	0.70 ± 0.01	1.240 ± 0.004
$\alpha \left[\frac{\lambda^2}{T} \right]$	-0.0285 ± 0.0014	-0.0282 ± 0.0006
$\beta \left[\frac{\lambda^2}{T} \right]$	0.0030 ± 0.0002	0.00470 ± 0.00006

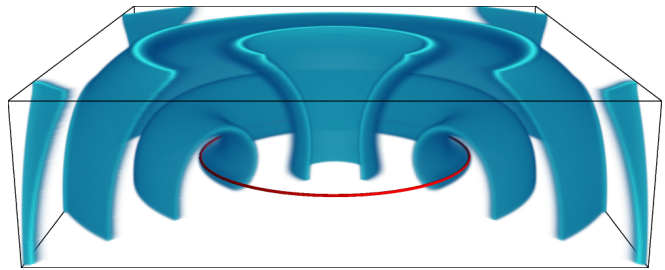


Figure 4. Schematic snapshot of a scroll ring within interaction distance to the lower Neumann boundary. In blue is shown the iso-concentration planes for one of the model variables and in red the ring-shaped filament.

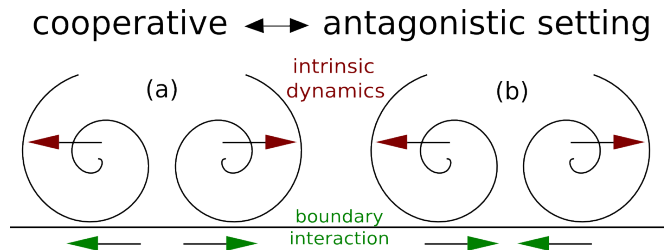


Figure 5. Cooperative (a) and antagonistic (b) setting for a scroll ring at a plane Neumann boundary. Intrinsic and boundary-induced dynamics indicated by full and dotted arrows, respectively.

IV. SCROLL RING INTERACTING WITH A NEUMANN BOUNDARY

To investigate how the interaction with a Neumann boundary influences the dynamics of an expanding scroll ring, we initiated scroll rings for chosen parameter sets as is illustrated in Fig. 1 for bounded media.

Fig. 4 shows an example for such a scroll ring that is displaying the isosurfaces of a scroll ring interacting with the lower Neumann boundary. The distance was chosen to be smaller than the distance at which a two dimensional spiral starts to interact with a Neumann boundary for the chosen parameters.

The interaction of a scroll ring with a Neumann boundary can either increase or decrease its radius. For a scroll ring that is intrinsically expanding both changes of the radius (due to intrinsic dynamics and boundary interaction) have the same sign. This setting we will indicate as cooperative (Fig. 5a), while the second case, where boundary interaction has the opposite effect on the radius evolution, we will correspond to as antagonistic setting (Fig. 5b).

The example scroll ring (Fig. 4) interacts with the lower boundary in an antagonistic setting. Such a scroll ring does not expand but shrink (Fig. 6) until it reaches a mean stationary radius \bar{R} and a mean stationary z -position \bar{z} (besides of the oscillation due to the filament

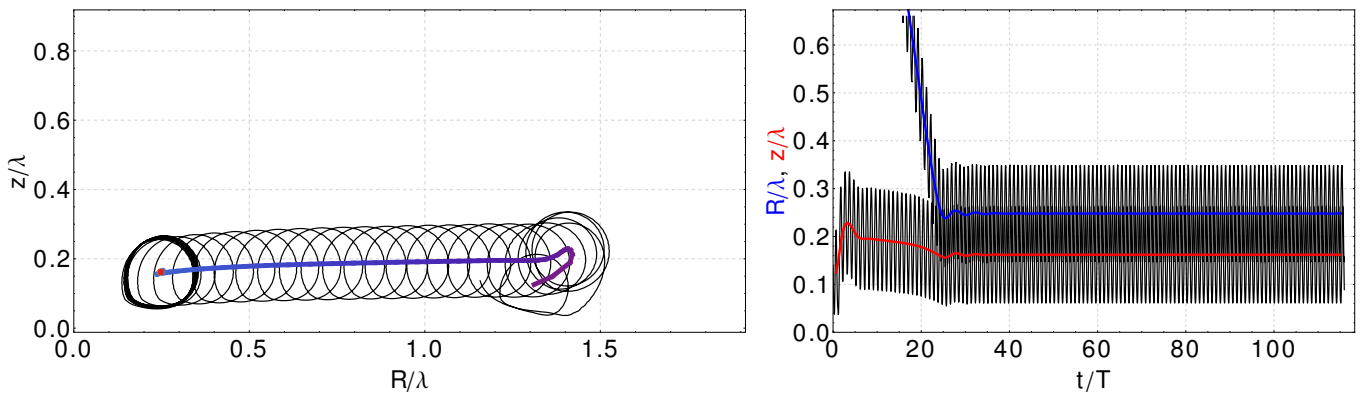


Figure 6. Plots for radius R over the z -coordinate (left) and R and z over time t (right) for a scroll ring propagating in a bounded medium and parameter set 2. The blue and red curves on the right panel are the calculated means for the radius $\bar{R}(t)$ and mean z -coordinate $\bar{z}(t)$, respectively. Due to the interaction with the boundary a stable scroll ring of finite radius is formed while the negative filament tension instability is suppressed. Values for mean radius and z -position are $\bar{R} = 0.250 \pm 0.003 \lambda$, $\bar{z} = 0.155 \pm 0.003 \lambda$. Simulation conducted for parameter set 2.

definition). In Fig 7 time evolution of the boundary-stabilized scroll ring is presented by different snapshots and view modes. Obviously the ring is contracting until it has reached a stable radius and it remains stable up to 300 periods of the corresponding spiral wave.

This state is stable for very long times (more than 400 rotation periods of corresponding spiral wave). Here we only present the first 300 periods for the sake of comprehensibility. For additional data (e.g. graphs, videos, etc.) the interested reader is referred to the supplementary material to this paper.

The formation of a boundary-stabilized scroll ring can be understood qualitatively if additional terms are introduced in the kinematic equations for the filament radius and the drift (equations 2 and 3, respectively) that account for the boundary effects (see reference [30])

$$\frac{dR}{dt} = -\frac{\alpha}{R} + c_p(z) + c_n(R), \quad (6)$$

$$\frac{dz}{dt} = \frac{\beta}{R} + c_n(z) - c_p(R), \quad (7)$$

with general spiral drift velocity functions $c_p(x)$ and $c_n(x)$, depending on radius R and z -position of scroll ring filament, that is $x \in \{z, R\}$.

$c_p(z)$ could for example strengthen the intrinsic time evolution of filament (cooperative setting, Fig. 5a) or weaken/suppress it (antagonistic setting, Fig. 5b).

In order to quantify boundary interaction of scroll rings and find corresponding spiral drift velocity fields c_p and c_n , we investigated systematically the interaction of a spiral wave in two spatial dimensions at a plane Neumann boundary [30].

We initiated the spiral at different distances to the boundary and calculated the resulting drift velocities of

the corresponding spiral core in parallel and normal direction to the boundary. This is shown schematically in Fig. 8.

Results are shown in Fig. 9. As one can see, the absolute value of both drift velocity components are very small, as long as the spiral core is more than $\sim 0.3 \lambda$ away from the boundary. As the spiral core reaches regions between $0.2 - 0.3 \lambda$ away from the boundary, the absolute values of the two velocity components are strongly increasing. The parallel drift velocity component reaches a maximum absolute value of $|c_p| \approx 0.029$.

The calculated value of the scroll ring filament tension for parameter set 2 is $\alpha \approx -0.028$ (see table II). Imagine now the scroll ring in each radial cross-section to be formed of two counter-rotating spirals (as is displayed in Fig. 5). Thus, in each radial cross-section such counter-rotating double-spirals drift in direction to each other. This is the manifestation of the antagonistic setting shown in Fig. 5(b). Since the absolute value for the parallel drift velocity is almost equal to the absolute value of the ring filament tension, expansion of the ring is stopped while the ring is stabilized at the boundary.

V. FORMATION OF BOUNDARY-STABILIZED SCROLL RINGS IN AN EXCIATBLE MEDIUM - CONDITIONS FOR OBSERVATION IN THE PBZR

In the previous section we have shown that an intrinsically expanding scroll ring can be stabilized at plane Neumann boundaries. This could be explained phenomenologically by boundary-induced drift of spiral waves in two spatial dimensions.

But until now we investigated the topic at a more conceptual level without considering at least the most im-

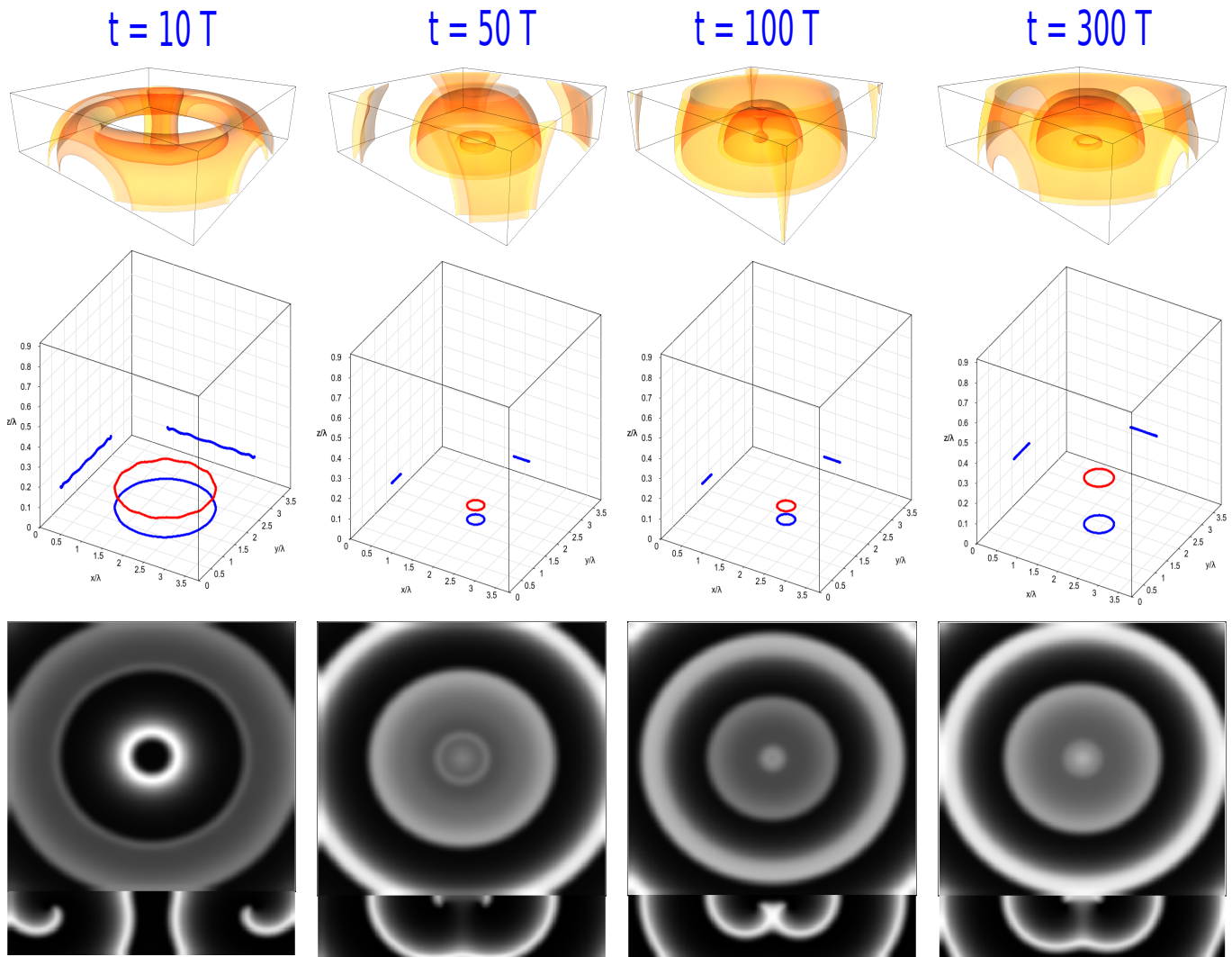


Figure 7. Multiple view panels for a scroll ring in a bounded medium: perspective, filament, top, and side view. (from top to bottom of figure). Perspective view displays the isosurfaces for Oregonator variable $u = 0.2$, filament view is showing the filament (red) and its projections into the different planes (blue), while the top view illustrates the overall concentration of Oregonator variable v as a sum over medium height (as may be seen by an observer of an experiment in the PBZR when looking from top). Figure displays stabilization of the filament at the boundary. Simulation conducted for parameter set 2.

portant deficiencies that are arising in real experimental systems.

In the next three subsections we will consider some important effects that come into play when working with photosensitive Belousov-Zhabotinskii reactions in thin gel layers loaded with silica and the catalyst Ruthenium [31, 32]. Effects that may hinder boundary-induced stabilization. In subsection V A we will examine first at which combinations of medium height and intensity of photoinhibition stable scroll rings can be initiated at all. Subsection V B will carry on with the question if boundary-induced stabilization is still possible at different degrees of inhomogeneity in z -direction. Finally, in subsection V C scroll rings will be initiated such that the filament plane will be inclined with reference to the boundary.

A. Initiation under variation of medium height and intensity of photoinhibition

In experiments with thin layers of photosensitive Belousov-Zhabotinskii media it is important to check whether boundary-stabilized scroll rings, as was presented in the previous section, can be initiated at all.

This is not trivial since two major problems have to be tackled. The first problem deals with the question for the minimum medium thickness to support formation of boundary-stabilized scroll rings. The second problem to solve comes with the photoinhibitory character of the system itself. As was already shown in references [23, 31], scroll rings can be initiated in the photosensitive BZ media by considering illumination of the medium in

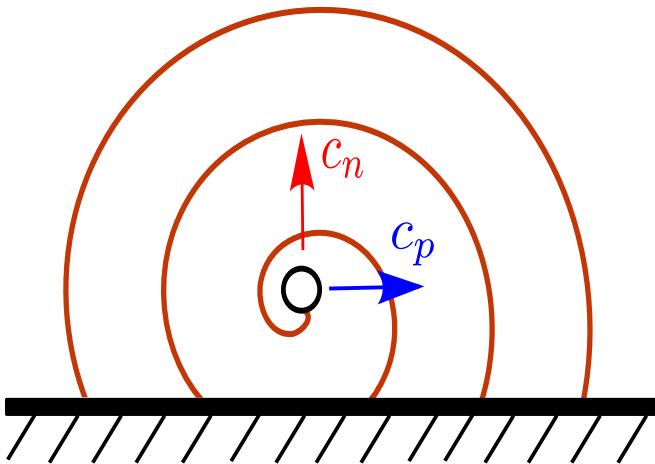


Figure 8. Sketch of a spiral at a plane Neumann boundary displaying boundary-induced drift velocities in parallel c_p and normal direction c_n to the boundary.

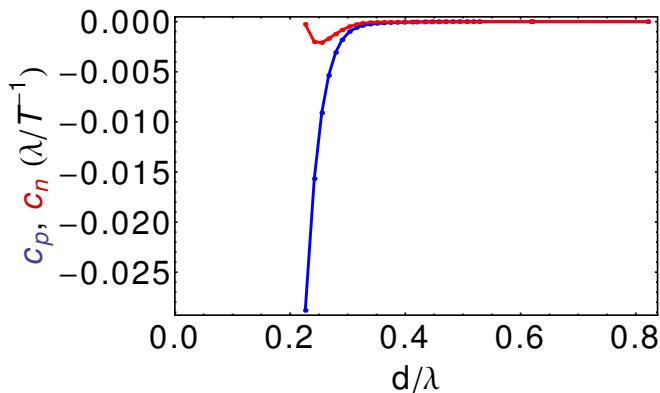


Figure 9. Calculated parallel and normal drift velocities, c_p and c_n respectively, for a spiral initiated at different distances from the boundary. Simulations conducted for parameter set 2.

the z -direction from above or below. The incident light is attenuated due to absorption in the medium. Thus, an illumination gradient in z -direction will be the consequence. Considering the photosensitive BZR this light gradient would lead to a gradient of inhibitor Br^- concentration in z -direction. Mathematically this light attenuation have been represented by the Lambert-Beer relation in the following sense:

$$\phi(z) = \phi_e \exp(-\alpha z), \quad (8)$$

when illumination from below is considered. This is the classic form of the Lambert-Beer relation that was also used in references [23, 31]. There α was introduced as a parameter that “includes the molar absorption coefficient and concentration of the reduced catalyst, $Ru(bpy)_3^{2+}$ ”, while the amplitude variable ϕ_e can be seen as “the quantum efficiency for the photochemical production of Br^- ”.

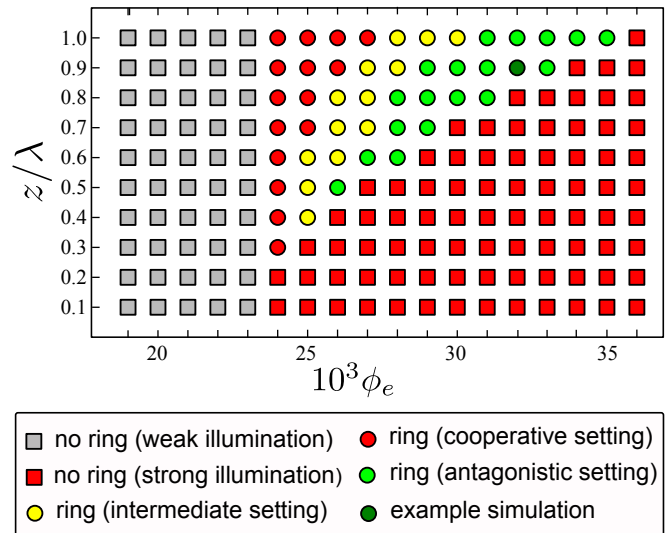


Figure 10. Numerical results for scroll ring initiation using partial inhibition of cylindrical wave fronts by external applied illumination. The photochemically induced bromide flow ϕ (which is assumed to be proportional to the acting light intensity) is set by the Lambert-Beer relation (equation 8) with $\phi_0 = 0.014$, $\alpha = 0.05$, while medium thickness and the illumination intensity parameter ϕ_e are varied.

In this work we fixed parameter α to the value $\alpha = 0.05$, while systematically varying thickness of media for chosen values of the illumination intensity parameter ϕ_e , in order to check for which value pairs of z and ϕ_e a stable scroll ring can be initiated. The high-intensity illumination that is represented by equation 8 will be turned on at time $t_{\text{start}} = 0 t.u.$ and turned off at time $t_{\text{end}} = 2 t.u.$ ($t.u.$ indicates simulation time units).

The results are shown in Fig. 10. In the complete region below $10^3 \phi_e = 24$ the overall illumination $\phi(z)$ was too weak for initiating stably rotating scroll rings. This is indicated by grey squares in the figure. For media with height values below 0.3λ (λ again is indicating the wave length of the corresponding spiral waves) the media are too thin to support formation of scroll rings, since illumination intensity values higher than $10^3 \phi_e = 24$ lead to complete inhibition of waves (indicated by red squares). Red circles represent formation of scroll rings that are interacting with one of the plane Neumann boundaries in a cooperative sense (see Fig. 5a). This would lead to an amplified expansion of the ring. Yellow circles denote scroll rings initiated such that their filament plane is located in the middle between the two boundaries. Such initiated rings may vertically drift to the stabilizing boundary (in the antagonistic setting shown in Fig. 5b). Finally, by green circles the truly boundary-stabilized scroll rings are represented. In these cases, the layer thickness as well as the illumination intensity are appropriate for initiating scroll rings that are from the start perfectly placed in the interaction regime to the stabi-

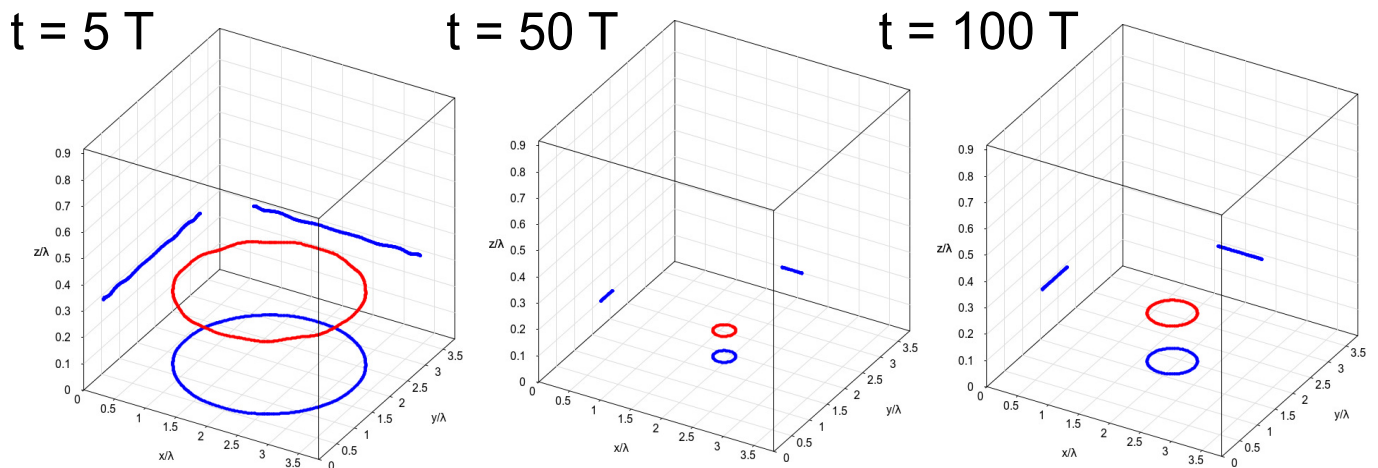


Figure 11. Evolution of the filament in the course of time for scroll rings in a gradient of the illumination parameter ϕ . Gradients accomplished by application of the Lambert-Beer law $\phi(z) = \phi_0 e^{-\alpha z}$ with $\phi_0 = 0.014$ and $\alpha = 0.0033$.

lizing boundary. A combination, by which the resulting ring would be analogous to the example case from previous section, is also shown here by a dark green circle.

B. Excitability gradient in parallel to scroll ring's symmetry axis

In the previous subsection we demonstrated how formation of boundary-stabilized scroll rings could be achieved in the framework of the photosensitive Belousov-Zhabotinskii reaction. This was done by setting up a temporarily inhomogeneous photoinhibition in z -direction based upon the Lambert-Beer relation, while the further time evolution of the scroll ring was accomplished under homogeneous illumination.

For testing stability of a boundary-induced pacemaker in a more realistic experimental situation one has to take into account spatially inhomogeneous illumination during the whole simulation time.

Here we took a very early state (after 2 rotation periods) of the scroll ring for parameter set 2, presented in section IV, as initial state for further investigation in an illumination gradient with two different gradient strengths. This was achieved by setting the light parameter ϕ inhomogeneously through the Lambert-Beer relation,

$$\phi(z) = \phi_0 \exp(-\alpha z)$$

from below, $\phi_0 = 0.014$, and two different absorption parameters, (1) $\alpha_1 = 0.0033$, and (2) $\alpha_2 = 0.01$.

Exemplarily, evolution of filament for absorption parameter 1 is shown in Fig. 11. For both gradient strengths the scroll ring is stable more than 400 rotation periods of the corresponding spiral wave. Here, for reasons of comprehensibility, evolution for the first 100 periods is shown.

As one can see also the shape of the scroll ring filament does not change much. This means that the scroll ring at the no-flux boundary acts as a periodic source of waves, at least over a relative long time.

C. Inclined initiation

Under some circumstances initiation of scroll rings in experiments for lightsensitive BZR may also happen inhomogeneously in horizontal (x - and/or y -) direction, such that scroll rings can not be initiated perfectly planar but in some way inclined.

Here we want to address the question if a boundary-induced stabilization nevertheless can be reached when a scroll ring is initiated in an inclined fashion, such that the initial phase of boundary interaction is not equal for different points of the corresponding ring-shaped filament.

To investigate inclined scroll rings numerically, we have chosen cylindrical-shaped waves as initial conditions, like it was done in the previous sections for planar scroll rings (see Fig. 1), but this time we initiated the inclined scroll rings by setting the Oregonator model parameter $\phi = \phi(x, z)$ according to the following function

$$\phi(x, z) = \phi_0 + \phi_e \exp(-\alpha z) + \frac{\phi_i}{L} x, \quad (9)$$

turned on at time $t_{\text{start}} = 0$ and turned off at time $t_{\text{end}} = 0.5$. Here the second term, characterized by parameters ϕ_e and α , is the well-known Lambert-Beer relation. These two parameters will be fixed, $\phi_e = 0.05$ and $\alpha = 0.1$. The last term introduces inclination of the final scroll ring. The degree and strength of inclination can be controlled by parameters ϕ_i , and L .

We conducted simulations for scroll rings at the antagonistic boundary with two different inclination states:

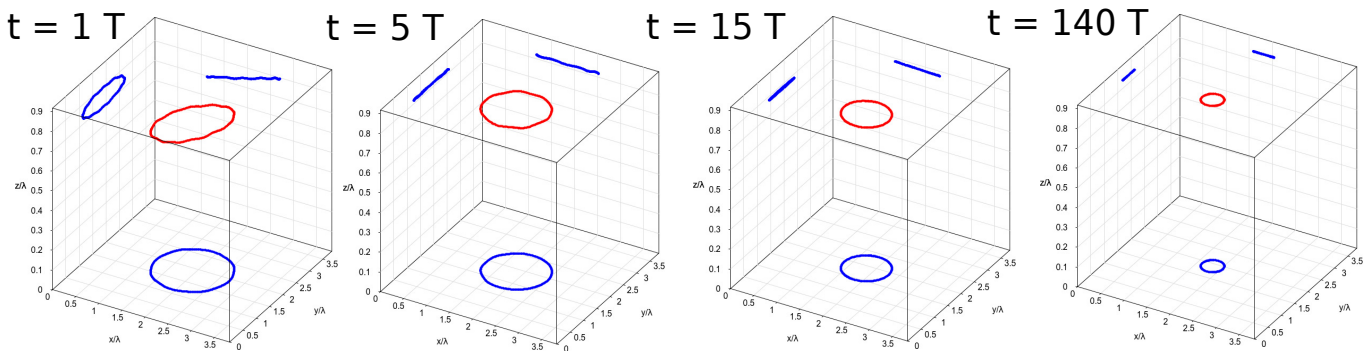


Figure 12. Evolution of an inclined scroll ring filament up to 140 rotation periods of the corresponding spiral wave. Different snapshots of the filament (red) with its projections on the sidewalls (blue) are shown. Initiation by application of the function 9 with $\phi_e = 0.05$, $\alpha = 0.1$, $\phi_i = 0.01$, and $L = 125$. Simulation carried out for parameter set 2.

$\phi_i = 0.01$ and (1) $L = 125$ and (2) $L = 100$. For case 1 the inclination angle relative to the boundary at time $t = 1T$ had a value of $\gamma_{\text{inc}} \approx 4^\circ$, while for inclination state 2 this value was $\gamma_{\text{inc}} \approx 5^\circ$. In both cases the scroll ring stabilized, up to 300 rotation periods of corresponding spiral wave. Exemplarily, this is shown for the inclination state 1 in Fig. 12. As one can observe here, the primarily inclined ring-shaped filament reaches a stable planar state already after 5 periods.

VI. CONCLUSION

We have shown that it is possible to stabilize an intrinsically expanding scroll ring via the interaction with a Neumann boundary. The negative line tension instability and Winfree-turbulence are suppressed, and instead the ring is stabilized. Finally, conditions were discussed under which scroll rings with negative filament tension could be stabilized in thin layers of the PBZR.

VII. ACKNOWLEDGEMENTS

We cordially thank the German Science Foundation (DFG) for financial support through the special research field 910 (sfb 910) and the Research Training Group 1558 (GRK 1558). Simulations in this paper were accomplished within the interactive reaction-diffusion simulation environment **VirtualLab** that was developed in our work group. Thus we thank the people (S. Fruhner, F. Paul, S. Molnos, D. Kulawiak, etc.) who helped us to build up this outstanding tool.

* azhand@itp.tu-berlin.de

[1] F. Siegert and C. J. Weijer, *Physica D* **49**, 37-72 (1991).

- [2] S. Jakubith, H. H. Rotermund and W. Engel and A. von Oertzen and G. Ertl, *Phys. Rev. Lett.* **65**, 3013-3016 (1990).
- [3] A. T. Winfree, *Science* **175**, 634-636 (1972).
- [4] J. M. Davidenko, A. M. Pertsov, R. Salomonsz, W. Baxter and J. Jalife, *Nature* **355**, 349-351 (1992).
- [5] I. Aranson, D. Kessler and I. Mitkov, *Phys. Rev. E* **50**, 2395-2398 (1994).
- [6] M. Gómez-Gesteira, A. P. Muñuzuri, V. Pérez-Muñuzuri, and V. Pérez-Villar, *Phys. Rev. E* **53**, 5480-5483 (1996).
- [7] V. M. Eguíluz, E. Hernández-García and O. Piro, *Int. J. Bifurcation Chaos* **9**, 2209-2214 (1999).
- [8] M. Bär, A. K. Bangia and I. G. Kevrekidis, *Phys. Rev. E* **67**, 056126 (2003).
- [9] A. T. Winfree, *Science* **181**, 934 (1973).
- [10] A. B. Medvinsky, A. V. Panfilov and A. M. Pertsov, in *Self-Organization: Autowaves and Structures Far From Equilibrium*, edited by V. I. Krinsky (Springer, Heidelberg, 1984), p. 195.
- [11] A. T. Winfree, *Sci. Am.* **230** (6), 82 (1974).
- [12] B. Welsh, J. Gomatam, and A. Burgess, *Nature* **304**, 611 (1983).
- [13] A. T. Winfree and W. Jahnke, *J. Phys. Chem.* **93**, 2823-2832 (1989).
- [14] T. Bánsági and O. Steinbock, *Phys. Rev. Lett.* **97**, 198301 (2006).
- [15] L. V. Yakushevich, *Studia Biophysica* **100** (3), 195-200 (1984).
- [16] J. P. Keener, *Physica D* **31**, 269-276 (1988).
- [17] V. N. Biktashev, A. V. Holden and H. Zhang, *Phil. Trans. R. Soc. A* **347** (1994).
- [18] A. V. Panfilov and A. N. Rudenko, *Physica D* **28**, 215 (1987).
- [19] T. Bánsági and O. Steinbock, *Phys. Rev. E* **76**, 045202(R) (2007).
- [20] S. Alonso, F. Sagues and A. S. Mikhailov, *Science* **299**, 1722-1725 (2003).
- [21] R. M. Zaritski, S. F. Mironov and A. M. Pertsov, *Phys. Rev. Lett.* **92**, 168302 (2004).
- [22] S. Alonso, F. Sagués, and A. S. Mikhailov, *Chaos* **16**, 023124 (2006).
- [23] T. Amemiya, P. Kettunen, S. Kádár, T. Yamaguchi and K. Showalter, *Chaos* **8**, 872 (1998).
- [24] M. Vinson, S. Mironov, S. Mulvey and A. Pertsov, *Nature* **386**, 477-480 (1997) *Nature* **386**, 477-480 (1997).

- [25] M. Vinson and A. Pertsov, *Phys. Rev. E* **59**, 2764 (1999).
- [26] P. J. Nandapurkar and A. T. Winfree, *Physica D* **35**, 277-288 (1989).
- [27] M.-A. Bray and J. P. Wikswo, *Phys. Rev. Lett.* **90**, 238303 (2003).
- [28] H.-J. Krug, L. Pohlmann and L. Kuhnert, *J. Phys. Chem.* **94**, 4862-4866 (1990).
- [29] S. Kádár, T. Amemiya and K. Showalter, *J. Phys. Chem. A* **101**, 8200-8206 (1997).
- [30] J. F. Tetz, H. Engel, O. Steinbock, *submitted* (2013).
- [31] T. Amemiya, S. Kádár, P. Kettunen, K. Showalter, *Phys. Rev. Lett.* **77**, 3244 (1996).
- [32] H. Linde and H. Engel, *Physica D* **49**, 13-20 (1991).